



13th International Conference on Greenhouse Gas Control Technologies, GHGT-13, 14-18  
November 2016, Lausanne, Switzerland

## 2.5D inversion and joint interpretation of CSEM data at Sleipner CO<sub>2</sub> storage

Joonsang Park<sup>a\*</sup>, Guillaume Sauvin<sup>a</sup>, Malte Vöge<sup>a</sup>

<sup>a</sup>Norwegian Geotechnical Institute (NGI), Sognsveien 72, 0855, Oslo, Norway

---

### Abstract

In this paper, we revisit the marine controlled-source electromagnetic (CSEM) data, acquired above the Sleipner CO<sub>2</sub> storage, in order to further study the dataset and conclude the feasibility of marine CSEM for offshore CCS monitoring. There are some challenges with respect to CSEM in this particular area: 1) strong airwave influence (due to regional shallow water depth); 2) potential of weak resistivity anomaly; 3) seabed pipeline network; and 4) rather shallow target depth. We are yet able to extract useful information; interpret further the CSEM inversion results by combining seismic data; and to extract the *in situ* resistivity and saturation of CO<sub>2</sub> in the Utsira formation by applying a rock physics model. In addition, to minimize the influence of the seabed pipeline on the CSEM data, we have muted some of data and receivers near the seabed pipeline network. The results show a good agreement with seismic data, and the estimated total mass of CO<sub>2</sub> agrees well with the injection data. This current study confirms that the marine CSEM can be an important and essential tool for offshore CO<sub>2</sub> storage monitoring, yet not alone but when combined with both seismic and gravity. Finally, near-future large-scale CCS projects in the North Sea would require extensive infra-structures such as seabed pipeline, etc. This study demonstrates that CSEM may work even with such infra-structures in place.

© 2017 The Authors. Published by Elsevier Ltd. This is an open access article under the CC BY-NC-ND license (<http://creativecommons.org/licenses/by-nc-nd/4.0/>).

Peer-review under responsibility of the organizing committee of GHGT-13.

**Keywords:** CCS, Sleipner, marine CSEM, monitoring, rock physics model

---

---

\* Corresponding author. Tel.: +47-932 12 453; fax: +47-2223 0448.  
E-mail address: [jp@ngi.no](mailto:jp@ngi.no)

## 1. Introduction

The Sleipner CO<sub>2</sub> storage is to date the longest-running Carbon Capture and Storage (CCS) project in the North Sea. Around 16 million-ton CO<sub>2</sub> has been injected successfully and stored safely at the depth of ca. 700 to 900 mbsb in the Utsira formation during the last two decades. For the geophysical time-lapse monitoring purposes, seismic and gravity data have been acquired almost every second or third year. Fig.1 shows two 2D seismic sections extracted from 3D volumes: one for year 1994 (pre-injection) and the other for year 2007 (during-injection). Seismic data is proven to delineate the distribution of the injected CO<sub>2</sub> in the Utsira formation. In addition to the CO<sub>2</sub> plume, the seismic data identify potential gas flows and pockets in the region. On the other hand, only a single controlled-source electromagnetic (CSEM) survey has been conducted in 2008 along one tow-line for research purpose (Project CO<sub>2</sub>ReMoVe). There are some challenges with respect to CSEM in this particular area (Park et al, 2011). For example, 1) the water depth is only around 80 m (strong airwave influence on CSEM data); 2) the injected CO<sub>2</sub> seems to show up as very weak resistivity anomaly (Alemu et al., 2012); 3) there is a pipeline network on seabed (which interferes with the CSEM data); and 4) rather shallow target detection via CSEM. Nevertheless, the current inversion study is able to extract the resistivity profile of the injected CO<sub>2</sub> in the Utsira formation by means of a 2.5D inversion algorithm (Vöge et al, 2014). The inversion algorithm is based on a Levenberg-Marquardt approach and the involved forward calculation engine is based on a 2.5D finite element method, which allows for anisotropic resistivity. The initial resistivity model and grid for the inversion are based on seismic data and available well-log in the area. Then, we attempt to further interpret the inversion results by combining the seismic data (for layering/geometry constraint) and a rock physics model in order to extract the *in situ* resistivity, saturation and mass of the injected CO<sub>2</sub> in the Utsira formation. The current study is a continuation of the previous studies (Park et al., 2013; Park et al. 2014) with application of the more advanced EM inversion algorithm.

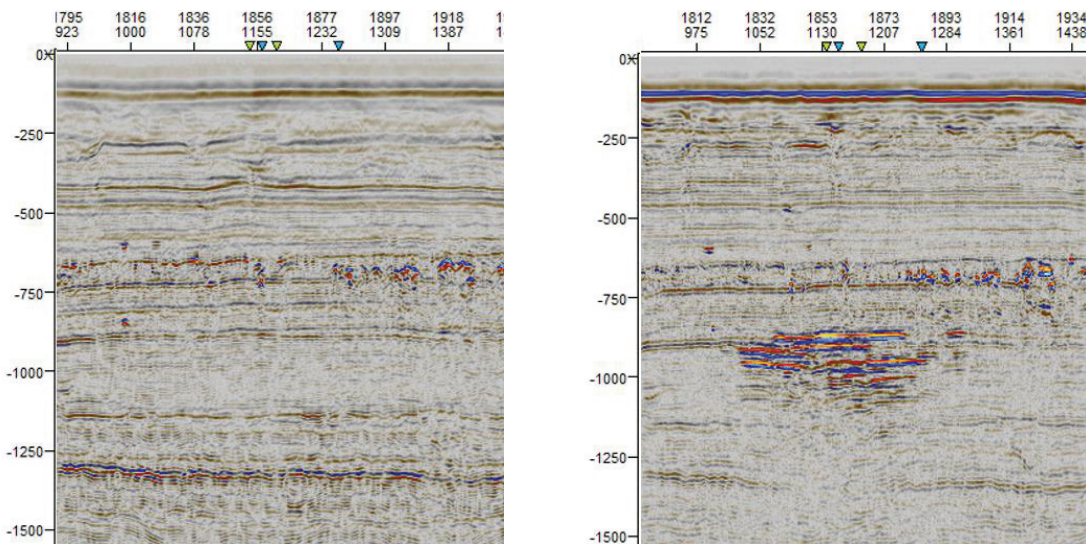


Fig. 1. Seismic images in time for pre-injection in 1994 (Left) and during-injection in late 2007 (Right). The images are taken from the vertical section along the CSEM survey line (See Fig. 2) [Seismic data is provided by Statoil].

## 2. 2008 CSEM survey and data in Sleipner

The CSEM data was acquired just above the area of the CO<sub>2</sub> plume in September 2008 (See Fig. 2). The survey was done along a single line and the EM source (horizontal dipole source, HED) was towed just above the seabed. 27 receivers were deployed on the seabed with around 500m spacing, and few of them were just to each other. The towline was stretched by around 10km further outside the receiver array. Namely, the total length of the towline was around 30km. The right plot in Fig. 2 shows the survey layout (green dots and line) together with the seabed pipeline network (brown lines). Both of the inline electric and broadside magnetic fields were acquired. In the current study, only the inline electric field is used. The available frequencies are 0.5, 1.0, 1.5, 2.0, 2.5 and 7.0 Hz. As shown in Fig. 2, the seabed pipelines cross the survey line at 6 different places, which causes strong interference with the EM data.

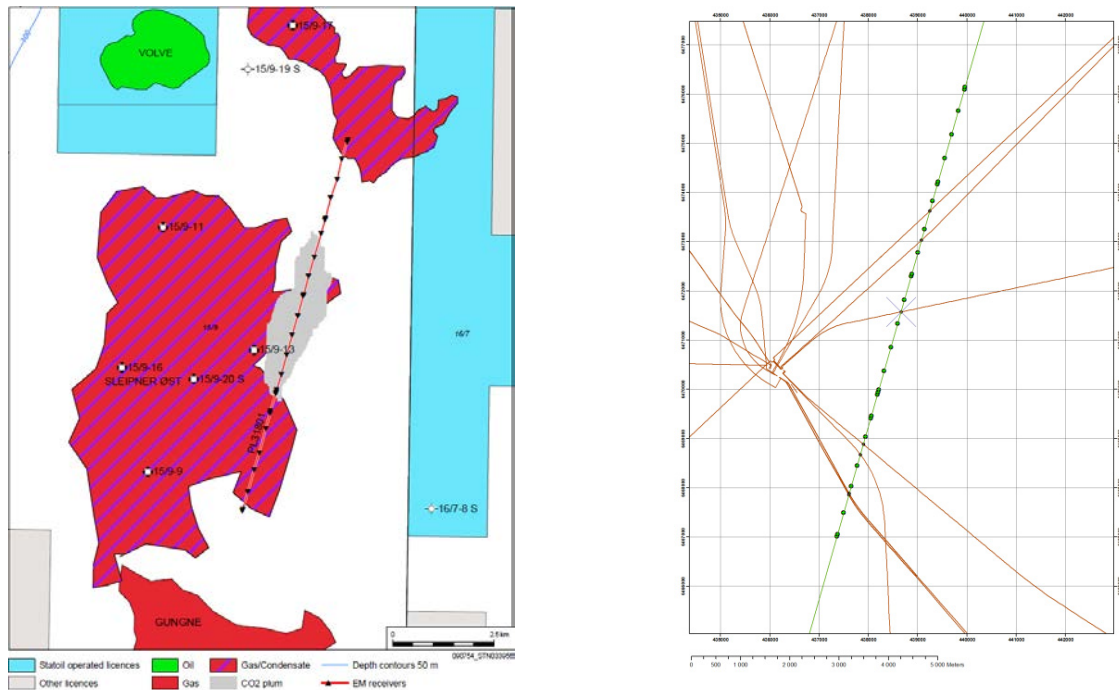


Fig. 2. (Left) CSEM survey layout (black dots and red line) shown on the Sleipner area map; (Right) seabed pipes (brown lines) crossing the CSEM survey line (green dots and line). The black and green dots correspond to the receiver locations. [provided by Statoil] (Park et al, 2013)

Fig. 3 shows all the inline electric fields at two different frequencies of 1.0 and 2.0Hz, together with the positions of all the 27 receives (yellow triangles) and pipelines (red circles). The quality of the EM data is excellent, e.g. low noise level except at very near offset. However, it is clearly shown that the data interferes strongly with the seabed pipelines, particularly with the two pipelines at  $6000m \leq x \leq 7000m$ . The other pipelines also show some interference, but much less. The interference depends on the size of the pipes but also (perhaps more importantly) the angle between the pipeline and the survey line, i.e. the smaller angle, the stronger the interference. In addition, according to Fig. 3, some of the receivers that are located very close to each other show almost the same data behaviors. Therefore, we used 20 (or 14 for the case of muting data w.r.t. pipelines) receivers in our inversion study. Finally, it should also be noticed that the inline electric field starts decaying slowly from the offset of around 3km (i.e. less attenuation), which is the indication of the significant airwave influence.

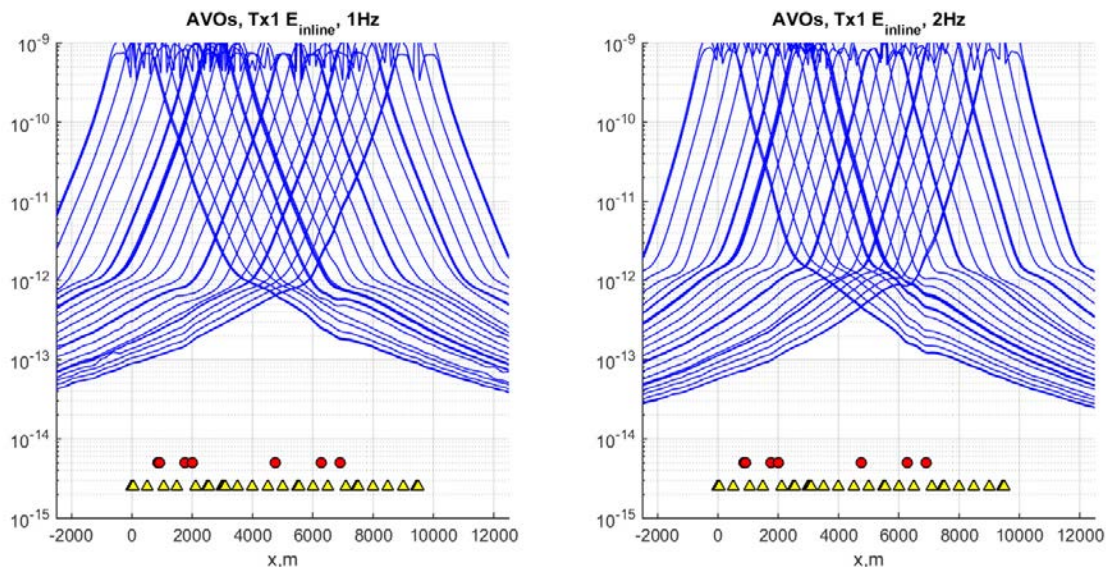


Fig. 3. Example of Sleipner CSEM data (inline electric field,  $E_{inline}$ ): (Left: 1Hz; Right: 2Hz) shown together with crossing seabed pipelines (red circles) and seabed receivers (yellow triangles). Note that six frequencies of 0.5, 1.0, 1.5, 2.0, 2.5 and 7.0Hz are available in the dataset, all of which are included into the inversion.

### 3. CSEM data inversion

For the inversion, we consider all the six frequencies of 0.5, 1.0, 1.5, 2.0, 2.5 and 7.0 Hz that are available from the acquisition. However, we use only 20 receivers out of 27, because some of them are very close to each other, showing almost the same behavior. Namely, Rx002a, Rx008a, Rx009a, Rx011a, Rx017a, Rx022a, and Rx026a are removed from the inversion setup. In addition, we use the offset range of 1000m-8000m for all the six frequencies and 300m spacing between data points. Both the amplitude and phase of the inline electric field ( $E_{inline}$ ) are inverted. The measured broadside magnetic field is available but not included in the current inversion study, which is an on-going activity. The initial resistivity model and grid for the inversion are based on seismic data and available well-log in the area but as rather loose constraint. For a given inversion initial model and grid, we consider two different cases: one without muting any data w.r.t. the pipelines and the other with muting. Accordingly, for the latter, Rx005a, Rx006a, Rx018a, Rx019a, Rx020a, and Rx021a are further removed from the inversion setup. The data muting is done manually simply by looking at the amplitude and phase versus offset curves (AVOs and PVOs), which is feasible with the current dataset (not too extensive). Fig. 4 shows the inversion results for the two cases of without (upper) and with (lower) muting data w.r.t. the pipelines in terms of the vertical resistivity ( $\log_{10}(\rho_v)$  [ $\Omega\text{m}$ ]). The two inversion results show both similarities and differences. For the depths of  $<500\text{m}$  and  $>1250\text{m}$ , the inversion results look rather similar. On the other hand, for the depths of  $>500\text{m}$  and  $<1250\text{m}$ , the inversion result with muting data shows more geologically-sensible resistivity model than that without muting data. For example, the latter shows strong inclined features in the resistivity at the distance between 13km and 20km, which is believed to be non-geological feature and be the influence of the seabed pipeline on the inversion result.

Fig. 5 shows the inversion results for the case of muting data w.r.t. seabed pipeline in terms of both of the vertical resistivity ( $\rho_v$ ) and the anisotropic ratio ( $\rho_v/\rho_h$ ), overlapped over the seismic image for late 2007. Note that the seismic image is in time and the EM inversion is in depth. The two images are manually adjusted to match each other, by

means of which we can see good agreement between the seismic image and the EM inversion results on the CO<sub>2</sub> plume location, from both of the vertical resistivity ( $\rho_v$ ) and the anisotropic ratio ( $\rho_h/\rho_v$ ). Of course, it is noted that the EM resolution is too low to resolve fully the detailed layering and exact depth of the CO<sub>2</sub> plume as imaged by the seismic. On the other hand, it is shown that the lateral extension of the CO<sub>2</sub> plume is well captured by the EM data inversion. It should also be noticed that there is another resistivity anomaly to the right above of the CO<sub>2</sub> plume, which is believed to be related to the potential air/gas pockets in the upper layer above the Utsira formation, not related to any leakage of the injected CO<sub>2</sub>. This can also be confirmed from the two seismic sections shown in Fig. 1. The two seismic sections have both the bright spots in the same area, and many more different places but smaller sizes.

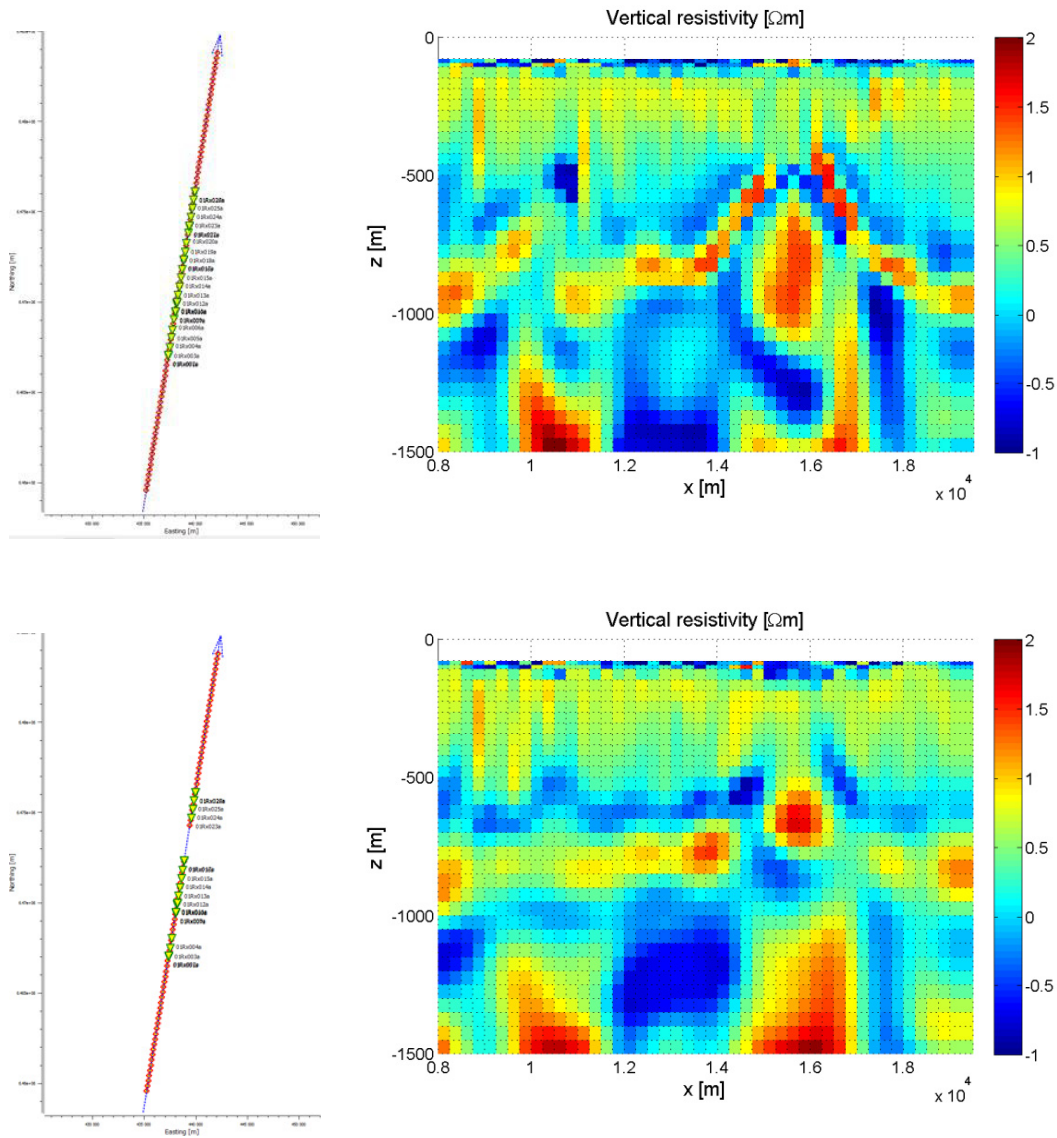


Fig. 4. Data/receivers in use (Left column) and inversion results in terms of vertical resistivity ( $\rho_v$ ) (Right column): inversion without muting any data (Upper row); inversion with muting data w.r.t. pipeline (Lower row)

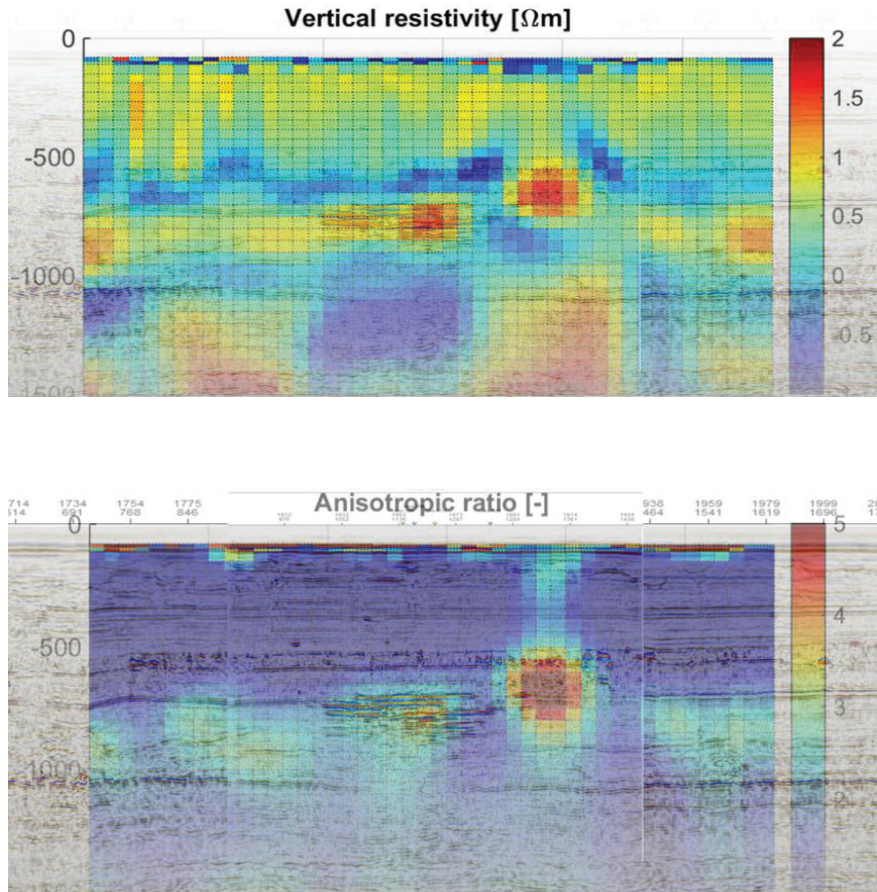


Fig. 5. Inversion results of vertical resistivity ( $\rho_v$ ) and anisotropic ratio ( $\rho_v/\rho_h$ ) shown over the seismic images from late 2007.

#### 4. Further interpretation

Now we attempt to estimate the saturation of CO<sub>2</sub> ( $S_{CO_2}$ ) based on the inversion results shown earlier and by using a simple rock physics approach, where we apply an averaged anisotropy medium assumption and the Archie's law (Archie, 1942). As shown earlier in the seismic section and literature (e.g. Arts et al, 2008), the CO<sub>2</sub> plume in the Sleipner field is accumulated at different depths within the Utsira formation due to several mudstone interlayers. The seismic captures those layers, but the CSEM does not (due to its low resolution). Instead, the CSEM data shows the CO<sub>2</sub> plume layers as few larger-volume anomalies, which is the same for the potential gas pockets (to the right above of the CO<sub>2</sub> plume). Furthermore, the larger-volume anomalies are indicated not only as high resistive anomalies, but also as high anisotropic anomalies. This observation leads us to consider the approach of averaged anisotropy medium. Namely, the EM inversion provides us with the averaged vertical and horizontal resistivities per grid of  $\rho_v$  and  $\rho_h$ , not directly the resistivities of the CO<sub>2</sub> plume layers ( $\rho_{CO_2}$ ) and the background Utsira formation ( $\rho_{back}$ ). From the seismic image, we may estimate the fractions of the CO<sub>2</sub> plume layers ( $f_{CO_2}$ ) and the background formation ( $f_{back}$ ). In the current study, we take  $f_{CO_2}=0.1$  and  $f_{back}=0.9$ . Then, we can estimate  $\rho_{CO_2}$  and  $\rho_{back}$  by means of the following formulas.

$$\rho_v = f_{back}\rho_{back} + f_{CO2}\rho_{CO2} \text{ and } \frac{1}{\rho_h} = \frac{f_{back}}{\rho_{back}} + \frac{f_{CO2}}{\rho_{CO2}} \tag{1}$$

Once knowing  $\rho_{CO2}$  and  $\rho_{back}$ , we can estimate further the saturation of CO2 by means of the Archie's law (Step 3 in Fig. 6). The procedure is summarized schematically in Fig. 6. Note that the procedure is applied to inversion grid by inversion grid whose size is 50m×250m×800m. Note that the width of 800m is assumed based on the seismic data or the plume extend shown in Fig. 2.

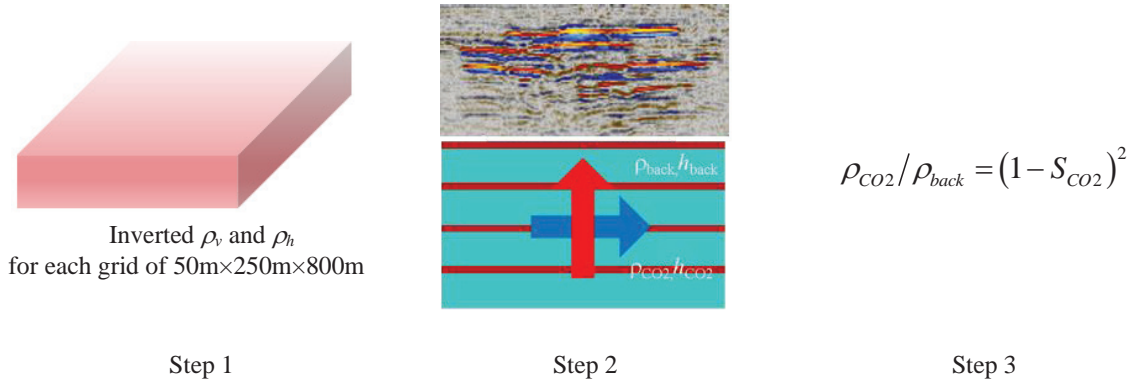


Fig. 6. Procedure to estimate the saturation of CO2 ( $S_{CO2}$ ) based on the CSEM inversion. Note that the procedure is applied to each inversion grid of 50m×250m×800m.

Fig. 7 shows all the inversion grids by filling each with the estimated CO2 saturation ( $S_{CO2}$ ). Note that the inversion grids shown in Fig. 7 are selected among all the inversion grids by comparing the inversion results with the seismic sections. Note that the depth range of the CO2 plume in Fig. 7 is from -700m to -900m (from the sea surface), not -800m to -1000m, which shows one of the features of the CSEM data (i.e. lower resolution in the depth direction than the lateral resolution).

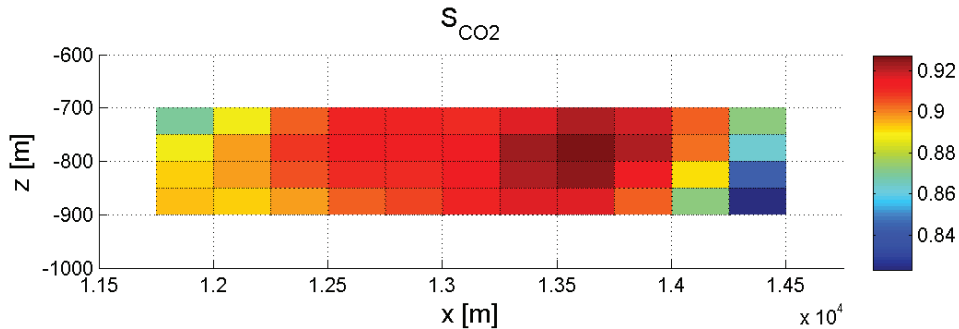


Fig. 7. CO2 saturation ( $S_{CO2}$ ) distribution obtained by the 3-step procedure.

Now we can also estimate the mass of the CO2 in the plume by means of the following simple formula:

$$M_{CO2} = \sum_{\text{inversion grid}} \rho_{CO2}\phi S_{CO2}V \tag{2}$$

where  $\rho_{CO_2}$  (CO<sub>2</sub> density) is assumed 700kg/m<sup>3</sup>,  $S_{CO_2}$  is taken from Fig. 7,  $\phi$  (Utsira porosity) is also assumed 0.37, each grid volume ( $V$ ) is 50m×250m×800m. The final result is then  $M_{CO_2}$ =10.3 million-ton, which agrees well with the total injected CO<sub>2</sub> by the time of the 2008 CSEM survey, i.e. early September, (Hagen, 2012).

## 5. Conclusions

This current study presents a new 2.5D inversion result of the Sleipner CSEM data acquired in 2008. The result supports that there seems to be no sign of CO<sub>2</sub> leakage through the cap rock and overburden. The study also confirms that the marine CSEM can be an important and essential tool for offshore CO<sub>2</sub> storage monitoring, particularly when combined with seismic and, perhaps, also gravity. Finally, near-future large-scale CCS projects in the North Sea would require extensive infra-structures such as seabed pipeline, etc. This study demonstrates that CSEM can work well even with such infra-structures during monitoring.

## Acknowledgements

The study is sponsored by FME centre SUCCESS for CO<sub>2</sub> storage under grant 193825/S60 from Research Council of Norway (RCN) and NGI. The CSEM data and other geophysical information are provided by the CO<sub>2</sub>ReMoVe project and Statoil. We also thank to the current and previous members of the NGI EM software consortium (Det Norske Oljeselskap ASA, Statoil ASA, Pure E&P (former Rocksource), CGG) for their support.

## References

- [1] Alemu, B., Aker, E., Soldal, M., Johnsen, Ø., and Aagaard, P. [2012] Effect of sub-core scale heterogeneities on acoustic and electrical properties of a reservoir rock: a CO<sub>2</sub> flooding experiment of brine saturated sandstone in a computed tomography scanner, *Geophysical Prospecting*.
- [2] Archie, G.E. 1942. The Electrical Resistivity Log as an Aid in Determining Some Reservoir Characteristics.
- [3] Arts, R., Chadwick, A., Eiken, O., Thibeau, S. and Nooner, S. [2008] Ten years' experience of monitoring CO<sub>2</sub> injection in the Utsira Sand at Sleipner offshore Norway, *First Break*, 26, 65-72.
- [4] Bickle, M., Chadwick, A., Huppert, H.E., Hallworth, M., and Lyle, S. [2007] Modelling carbon dioxide accumulation at Sleipner: Implications for underground carbon storage, *Earth and Planetary Science Letters*, Vol. 255, pp164-176.
- [5] Hagen, S. [2012] Sleipner - Knowledge sharing in CCS projects, Workshop Mobile, Alabama, May 16-17.
- [6] Park, J., Viken, I., Bjørnarå, T.I. and Aker, E. [2011]. CSEM data analysis for Sleipner CO<sub>2</sub> storage. Trondheim CCS-6 Conference, June 14-16, Trondheim, Norway.
- [7] Park, J., Fawad, M., Viken, I., Aker, E. and Bjørnarå, T.I. [2013] CSEM sensitivity study for Sleipner CO<sub>2</sub>-injection monitoring, *Energy Procedia*, Volume 37, pp. 4199-4206.
- [8] Park, J., Vanneste, M., Bohloli, B., Viken, I., Bjørnarå, T.I. [2014] In situ resistivity of CO<sub>2</sub> plume at Sleipner from CSEM and gravity data, Fourth EAGE CO<sub>2</sub> Geological Storage Workshop, 22-24 April 2014, Stavanger, Norway.
- [9] Soldal, M., Park, J., Lamech, L.O., Tran, T., Sauvin, G., Johnsen, Ø., and Mondol, N.H. [2015] Geophysical Monitoring of CO<sub>2</sub> Flow During Sandstone Flooding Experiments, 3rd EAGE Workshop on Rock Physics, Istanbul, Turkey on 15-18 November 2015.
- [10] Hagen, S. [2012] Sleipner - Knowledge sharing in CCS projects, Workshop Mobile, Alabama, May 16-17.
- [11] Vöge, M., Park, J., and Viken, I. [2014] Multi-line 2D Inversion of Marine CSEM data using 3D Regularization, Extended Abstract for 22nd EM Induction Workshop, Weimar, Germany, August 24-30, 2014.